Symmetrized mean-field description of magnetic instabilities in κ-(BEDT-TTF)$_2$Cu[N(CN)]$_2$Y salts

A. Painelli and A. Girlando

Dipartimento di Chimica Generale ed Inorganica, Chimica Analitica, Chimica Fisica, Università di Parma,
Parco Area delle Scienze, I-43100, Parma, Italy

A. Fortunelli

Istituto di Chimica Quantistica ed Energetica Molecolare del CNR, v. V. Alfieri 1, I-56010, Ghezzano (PI), Italy

We present a convenient mean-field method, and apply it to study the metallic/antiferromagnetic interface of κ-(BEDT-TTF)$_2$Cu[N(CN)]$_2$Y organic superconductors (BEDT-TTF is bis-ethylendithio-tetrathiafulvalene, $Y=$Cl,Br). The method, which fully exploits the crystal symmetry, allows one to obtain the mean-field solution of the two-dimensional Hubbard model for very large lattices (typically 6×10^5 sites), yielding a reliable description of the phase boundary in a wide region of the parameter space. The metal/antiferromagnet transition appears to be second order, except for a narrow region of the parameter space, where the transition is very sharp and possibly first order. The coexistence of metallic and antiferromagnetic properties is only observed for the transient state in the case of smooth second order transitions. The relevance of the present results to the complex experimental behavior of centrosymmetric κ-(BEDT-TTF)$_2$Cu[N(CN)]$_2$Y salts is discussed.

I. INTRODUCTION

The κ-phase (BEDT-TTF)$_2X$ salts exhibit a great variety of physical properties as a function of temperature, pressure, anion (X) substitution, deuteration, and even disorder in the ethylene end groups. Superconducting (SC), antiferromagnetic (AF), metallic, and insulating phases are observed.[1,2] Of particular interest is the AF/SC/metal borderline, which for κ-(BEDT-TTF)$_2$Cu(NCS)$_2$ and κ-(BEDT-TTF)$_2$Cu[N(CN)]$_2$Y ($Y=$Cl, Br; hereafter ET-Y family) occurs in a very narrow region of the temperature-pressure (T,p) space. For the aforementioned compounds, a schematic zero temperature phase diagram can be drawn as shown in Fig. 1.[3–5]

The proximity of SC and AF phases, together with other experimental evidence, suggested a possible role of spin fluctuations in the superconductivity mechanism,[5,6] and prompted intensive theoretical investigation on the SC/AF borderline.[5–11] Since the early suggestion by Kino and Fukuyama,[3,12] mean-field (MF) approaches have often been adopted to investigate the SC/AF interface.[8,9,11] Several previous MF treatments considered low-symmetry structures,[3,8,12] namely, κ-(BEDT-TTF)$_2$Cu(NCS)$_2$, with four inequivalent molecules in the unit cell. The resulting numerical calculation is complex and computationally very demanding, so that only fairly small lattices have been considered, leading to large intrinsic uncertainties on the estimated properties, particularly at the phase transition. On the other hand, in the orthorhombic centrosymmetric κ-phase crystals of the ET-Y family all molecules in the layer are equivalent.[13,14] The greater symmetry with respect to κ-(BEDT-TTF)$_2$Cu(NCS)$_2$ apparently does not lead to significant differences in the physical behavior, notably in the SC properties. Indeed, ET-Br is a superconductor at ambient pressure, and ET-Cl under moderate pressure presents the

highest T_c observed in (BEDT-TTF)$_2X$ salts.[2] The MF approach has been applied[9,11] also to these more symmetric lattices to study the coexistence of charge ordering instabilities. Including the order parameters relevant to charge instabilities further increases the complexity of the calculation and leads to large uncertainties in the transition region, as recognized by the authors of Ref. 9. We instead propose to fully exploit the higher symmetry of the centrosymmetric ET-Y structures to build a *symmetrized* MF approach for the superconducting metallic/magnetically ordered phase transition.[10] By exploiting symmetry we are able to work on lattices as large as 6×10^5 sites, and to explore a wide region of the parameter space, keeping numerical procedures and finite-size effects under control. Moreover and most importantly, we get a simple and complete description of the electronic bands of these system, focusing only on those effects which are directly connected with the interesting physics. The MF treatment maps the problem of interacting electrons into an effective noninteracting Hamiltonian. The comparison between reliable MF results and available experimental data then allows us to safely define the intrinsic limitations of effective one-electron pictures in describing the physics of κ-phase salts.

Recently more refined approaches have been applied to κ-phase salts. For instance, fluctuation-exchange (FLEX)[15,16]
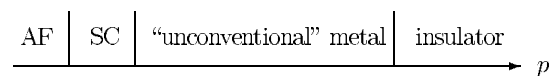

FIG. 1. Universal zero temperature phase diagram for κ-phase BEDT-TTF salts.

or third-order perturbation (PT) approach[17] have been applied to investigate the fluctuation mechanism for superconductivity and to estimate the critical temperature. However these approaches are only valid in the weak electronic correlations regime, and have been applied to a simplified model for the κ-phase layer, the so-called dimer model.[3,5,18,19] The same model has also been adopted in the framework of the dynamical MF[5,20] and within a renormalization group approach,[21] which offer complementary information with respect to ordinary MF techniques. As we shall discuss in the following, the reliability of the dimer model cannot be taken for granted in the whole parameter space. Here we show that by exploiting the high symmetry of the ET-Y salts family one can get a picture of the κ-phase layer that is computationally and theoretically as simple as the dimer model, without introducing any approximation.

In this paper we model the system in terms of a simple Hubbard t-U Hamiltonian, but the proposed procedure can be easily extended to t-U-V or t-J Hamiltonians, or to investigate charge-ordering transitions, whose possible coexistence with spin order has been recently suggested.[22] Moreover, the symmetry properties can be conveniently implemented in more refined calculation schemes, to get simpler and more reliable description of the physics of κ-phase salts. The paper is organized as follows. The next section is devoted to the description of the method. We then analyze the magnetic instabilities of ET-Y salts, and discuss the effects of the instabilities on the band structure. The difference between our symmetrized MF and other MF approaches is stressed, and the reliability of the dimer model is shortly addressed. Finally, we make connection with the experiment by discussing the pressure dependence of the SC/AF interface in the ET-Cl, and by making a comparison with ambient pressure ET-Br superconductor.

II. THE SYMMETRIZED MEAN FIELD APPROACH

Consistently with experimental data on centrosymmetric κ-phase salts,[13,14] we consider a unit cell with four equivalent molecular sites, and do not allow for modification of the periodicity of the crystal structure at the magnetic phase transition. We adopt the t-U Hubbard Hamiltonian to describe Coulomb interactions giving rise to magnetic ordering:

$$H = \sum_{\langle i,j \rangle \sigma} t_{ij}(a_{i\sigma}^\dagger a_{j\sigma} + \text{H.c.}) + \frac{U}{4} \sum_i n_i n_i - U \sum_i s_i s_i,$$
$$(2.1)$$

where the indices run on the BEDT-TTF sites, the first term accounts for the intersite hopping, and the other terms describe the on-site Coulomb repulsion. In Eq. (2.1), n_i is the usual site number operator $n_i = n_{i\uparrow} + n_{i\downarrow}$, and $s_i = (n_{i\uparrow} - n_{i\downarrow})/2$ is the net magnetization operator.

In the MF approximation the many-body interaction is described by an effective single particle interaction, where each particle feels the other particles as a source of a MF potential. Then each product of two electronic operators $\hat{A}\hat{B}$ is approximated with an expression where only a single operator appears, the effect of the second operator being sub-
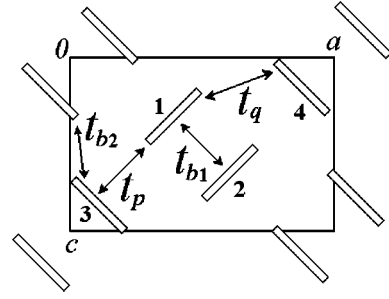

FIG. 2. Schematic view of the ac plane of centrosymmetric BEDT-TTF salts.

stituted by its ground-state expectation value. This approach gives reliable results when the fluctuations of the observables are small, although not zero as in single-particle approaches. Mathematically,

$$\hat{A}\hat{B} = (\langle A \rangle + \widehat{\Delta A})(\langle B \rangle + \widehat{\Delta B}) \approx \langle A \rangle \langle B \rangle + \langle A \rangle \widehat{\Delta B} + \langle B \rangle \widehat{\Delta A}.$$
$$(2.2)$$

Thus in MF the two-particle Hubbard terms of Eq. (2.1) become

$$\frac{U}{4} \sum_i n_i n_i - U \sum_i s_i s_i \simeq \frac{U}{2} \sum_i \langle n_i \rangle n_i - 2U \sum_i \langle s_i \rangle s_i.$$
$$(2.3)$$

The equivalence of the four molecular sites imposes the constraint

$$\langle n_{i\uparrow} \rangle + \langle n_{i\downarrow} \rangle = 1.5 \quad i = 1 \ldots 4. \quad (2.4)$$

Therefore the first term on the right-hand side of Eq. (2.3) is a constant, and the relevant physics is described by the net magnetization term. We rewrite it by exploiting symmetry, and define within each unit cell the following four order parameters:

$$\eta_{AF1} = (s_1 + s_2 - s_3 - s_4),$$

$$\eta_{AF2} = (s_1 - s_2 - s_3 + s_4),$$

$$\eta_{AF3} = (s_1 - s_2 + s_3 - s_4), \quad (2.5)$$

$$\eta_{FM} = (s_1 + s_2 + s_3 + s_4),$$

or, in short, $\eta_\nu = \Sigma_i c_i^\nu s_i$, with $\nu =$ AF1, AF2, AF3, FM. In these equations i counts the four BEDT-TTF sites within the unit cell, as indicated in Fig. 2. The order parameters η_{AF1}, η_{AF2}, and η_{AF3} correspond to the three possible antiferromagnetic orderings; η_{FM} describes the ferromagnetic phase. The net magnetization term in Eq. (2.3) then becomes $-2U\Sigma_i \langle s_i \rangle s_i = -(U/2)\Sigma_{j,\nu} \langle \eta_\nu \rangle \eta_\nu^{(j)}$, where j runs over the unit cells. Since translational symmetry is not broken by the magnetic transition, $\langle \eta_\nu \rangle$ is independent of j. The four magnetic phases have different symmetry, so that the four η_ν order parameters are orthonormal and can be investigated separately, leading to the symmetrized MF Hamiltonians

TABLE I. Hopping integrals and critical U for ET-Cl and ET-Br salts. All parameters in eV.

	t_{b1}	t_{b2}	t_p	t_q	U_c
ET-Cl, amb. p, $T = 127$ K	0.2315	0.0760	0.0901	0.0410	0.639 ± 0.001
ET-Cl, $p = 3$ Kbar, amb. T	0.2239	0.0851	0.0844	0.0517	0.676 ± 0.005
ET-Cl, $p = 27$ Kbar, amb. T	0.2770	0.0935	0.1400	0.0380	0.906 ± 0.005
ET-Br, amb. p, $T = 127$ K	0.2244	0.0712	0.0936	0.0396	0.636 ± 0.001

$$H_\nu = -\sum_{\langle l,k\rangle,\sigma} t_{lk}(a^\dagger_{l\sigma} a_{k\sigma} + \text{H.c.}) - Y_\nu \sum_j \eta_\nu^{(j)}, \quad (2.6)$$

where t_{lk} are the hopping parameters, i.e., t_{b_1}, t_{b_2}, t_p, and t_q defined in Fig. 2. For each symmetry, the effective single particle potential Y_ν is related to the expectation value of the relevant order parameter by the self-consistency equation

$$Y_\nu = \frac{U}{2} \langle \eta_\nu \rangle. \quad (2.7)$$

By rewriting the last term in Eq. (2.6) in terms of the original $n_{i\uparrow}$, $n_{i\downarrow}$ operators, one immediately recognizes that H_ν is the sum of two independent tight-binding Hamiltonians $H_{\nu\uparrow}$, $H_{\nu\downarrow}$, describing electrons with up and down spin, respectively. The off-diagonal part of each one of these Hamiltonians is exactly the same as in the original tight-binding model, but the MF treatment of on-site electron-electron interaction introduces a diagonal contribution. Specifically, the diagonal elements of $H_{\nu\uparrow}$ within each unit cell are

$$(H_{\nu\uparrow})_{ii} = -\frac{Y_\nu}{2} c_i^\nu \quad (2.8)$$

and $(H_{\nu\uparrow})_{ii} = -(H_{\nu\downarrow})_{ii}$. The two tight-binding problems described by $H_{\nu\uparrow}$ and $H_{\nu\downarrow}$ are easily diagonalized for different Y_ν values on very large lattices. In our approach imposing the self-consistency relation on U simply implies calculating the ratio between Y_ν and $\langle \eta_\nu \rangle$, at variance with the lengthy and memory consuming iteration steps required by a multi-parameter MF calculation.[3,8] This is very important in keeping the numerical procedure under control and allows us to work with very large lattices, typically up to 6×10^5 sites. Such large lattices, one order of magnitude larger than the largest lattice in Ref. 8, are diagonalized with no effort on a Digital Alpha 255 workstation equipped with 64 MB RAM. As we will discuss below, working on large lattices is very important to get an accurate description of the early stages of the phase transition, and then to get reliable information on the nature of the transition itself.

The diagonalization of $H_{\nu\uparrow}$, $H_{\nu\downarrow}$ immediately defines the band structures for up and down spins. In the case of the FM instability, all the c_ν^{FM} in Eq. (2.8) are equal to 1, so that, apart from a rigid shift of the energies by $-(+)Y_{\text{FM}}/2 = -(+)U\langle \eta_{\text{FM}} \rangle/4$ for up (down) spins, the eigenstates are exactly the same as in the noninteracting case. Therefore, the originally degenerate bands for up and down spins are split by $Y_{\text{FM}} = U\langle \eta_{\text{FM}} \rangle$. The Fermi level is fixed by the conservation of the total number of electrons, leading to unbalanced up and down spin population. If, without loss of generality,

we consider positive $\langle \eta_{\text{FM}} \rangle$, we end up with lower energies for up spins and then with a ferromagnetic state characterized by larger population of up than down spins.

In the case of AF order, instead, finite Y_ν deforms the original bands of the noninteracting system, due to the appearance of relevant diagonal terms in the real space Hamiltonian [Eq. (2.8)]. In this case, the eigenvalues for up and down spins are exactly the same, and the bands for the two spins stay exactly degenerate as in the noninteracting case, but the distribution of the two spin species is different on the sites, with a larger number of up spins residing on sites with negative c_i^ν coefficients ($\langle \eta_{\text{AF}} \rangle > 0$).

III. RESULTS

Table I summarizes the t's obtained from the available structural data of ET-Cl and ET-Br salts.[23,24] All t's have been obtained from extended Hückel (EH) calculations on the pairs of BEDT-TTF molecules corresponding to the four interactions depicted in Fig. 2. Specifically, they are evaluated as half of the splitting of the HOMO energy in each pair. It is well known that the values of the hopping integrals show large differences, depending on the method adopted for their estimate.[25] Therefore, the t's estimated for each structure and the resulting U_c have not to be assigned too much confidence. However, comparing results obtained with the same procedure on different structures is certainly informative. We have adopted EH estimates of t's since they compare well with available *ab initio* results.[26]

Figure 3 reports the Y_ν and U dependence of $\langle \eta_{\text{AF1}} \rangle$ and $\langle \eta_{\text{FM}} \rangle$ order parameters, as obtained for the t's relevant to ET-Cl at 127 K (first row in Table I). $\langle \eta_{\text{AF2}} \rangle$ and $\langle \eta_{\text{AF3}} \rangle$
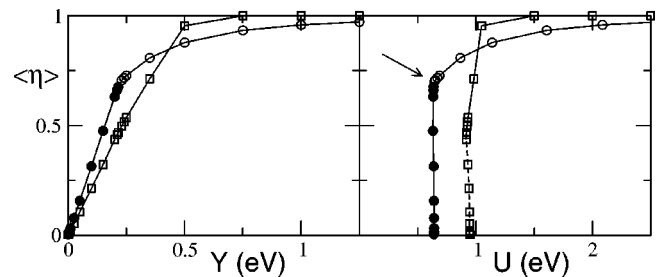
FIG. 3. ET-Cl at $T = 127$ K, ambient p: t's from the first row of Table I. The order parameter for FM instability (squares) and AF instability of type 1 (circles) vs the effective MF potential Y, in the left panel, and vs U in the right panel. Filled circles mark points introduced in the linear regression of the η vs Y to determine U_c (see text), the arrow marks the point where the conduction gap opens, and whose band structure is shown in Fig. 4, bottom panel.

curves are not shown since the corresponding instabilities occur at U larger than ~ 1 eV,[10] and are not relevant to our discussion. Indeed, even the ferromagnetic instability occurs at U higher than that for AF instabilities, and, in this respect, it is irrelevant from the physical point of view. However, the different behavior of $\langle \eta_{AF1} \rangle$ and $\langle \eta_{FM} \rangle$ in the right panel of Fig. 3 deserves some comments.

Based on the two standard stability conditions: $\partial E/\partial \eta = 0$ and $\partial^2 E/\partial \eta^2 > 0$, with E representing the expectation value of the working Hamiltonian, it is easy to prove that stable states for our system correspond to points with positive slope in the $\eta(U)$ curves.[27] The negative slope region in the $\eta_{FM}(U)$ curve (marked by a dotted line in the right panel of Fig. 3) then corresponds to unstable states, i.e., states that cannot be reached by our physical system. Thus the ferromagnetic instability corresponds to a first order phase transition, characterized by a discontinuous jump of the order parameter at the transition, located at $U_c \sim 0.945$ eV. The small region around U_c where the $\eta_{FM}(U)$ is non-single-valued corresponds to the hysteresis region, where two stable states coexist.

The behavior of $\langle \eta_{AF1} \rangle$ is different, with $\eta_{AF1}(U)$ having infinite slope at $U_c \sim 0.64$ eV. The infinite slope is a direct consequence of a strictly linear $\eta_{AF1}(Y_{AF1})$ dependence in a fairly large region around the origin. In Fig. 3, left panel, the filled circles show the points that fall on a single straight line, $\langle \eta_{AF1} \rangle = \chi Y_{AF1}$, with a squared correlation coefficient larger than 0.99998. By applying the self-consistency condition in Eq. (2.7), one immediately gets steeply increasing η_{AF1} values at a fixed $U = U_c = 2/\chi = 0.639$ eV. The coefficient $\chi = \partial^2 E/\partial Y_{AF1}^2$ represents the susceptibility of electronic system to the Y_{AF1} perturbation: the critical U is thus related to the inverse of the electronic susceptibility.

Extracting U_c from the slope of the $\langle \eta_{AF1} \rangle$ vs Y_{AF1} curve is a much safer procedure than searching for the minimum U where finite $\langle \eta_{AF1} \rangle$ appears. The calculated $\langle \eta_{AF1} \rangle$ values are affected by finite uncertainties, with a minimum intrinsic uncertainty given by the inverse of the number of unit cells. Since $\langle \eta_{AF1} \rangle$ enters the Hamiltonian matrix as a multiplicative factor for U, the uncertainty in $\langle \eta_{AF1} \rangle$ implies an uncertainty in U, with $\delta U/U = \delta \langle \eta_{AF1} \rangle / \langle \eta_{AF1} \rangle$. Therefore, at small $\langle \eta_{AF1} \rangle$ the relative uncertainty on U can be very large. This is by no means accidental, but reflects the intrinsic limitation of investigating phase transitions through finite size calculations. At the transition in fact the correlation length of the fluctuations in the order parameters are in principle infinite, so that calculations on finite lattices lead to large errors.

It is interesting to investigate the evolution of the electronic bands along the AF transition. Figure 4 reports the band structure calculated for the noninteracting metallic system, and for a system located just where the transition goes to completion, i.e., the point marked by an arrow in Fig. 3. The two conduction bands, that are partly overlapped in the metallic system, are split apart in the AF phase, opening a gap and then leading to insulating behavior. Figure 5 reports the U dependence of the energy difference between two extreme points in the two conduction bands (specifically between the M point in the upper band and the X point in the lowest conduction band) to measure the conductivity gap Δ.
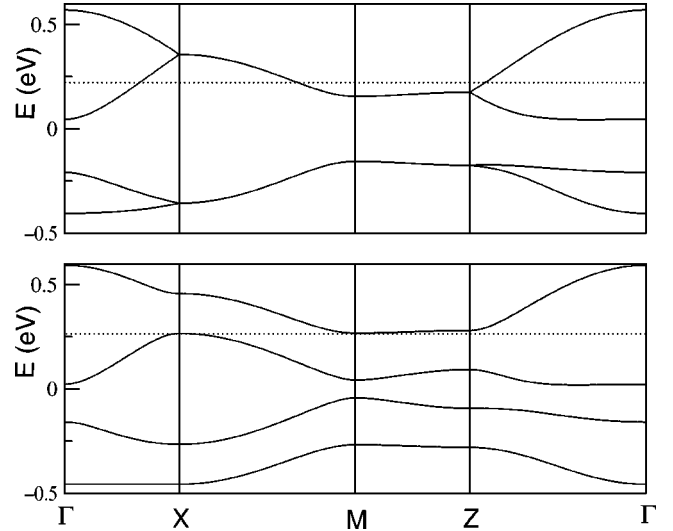

FIG. 4. Band structure for ETCl, same parameters as in Fig. 3. The upper panel refers to the noninteracting system (or equivalently to the system before the transition), the bottom panel corresponds to the point marked by an arrow in Fig. 3, $Y = 0.225$ eV. The dotted line marks the Fermi energy.

Negative Δ implies overlapping bands and then metallic behavior, positive Δ measures the semiconducting gap.

In summary, for the t's in the first row of Table I, relevant to ET-Cl at ambient pressure and $T = 127$ K, we observe a fairly sharp transition, at $U_c = 0.639$ eV, from a paramagnetic metal to an antiferromagnetic insulator, as shown by the semiconducting gap that opens up right at the transition (Fig. 5). In our approach the metallic phase includes the superconducting state, since our Hamiltonian does not account for SC coupling. The critical U is similar to available experimental[5,28] and theoretical[26] estimates of the effective U in BEDT-TTF salts, $U \sim 0.5$–1.0 eV. Therefore ET-Cl is just located at the metal/AF interface, in agreement with several experimental observations (see below). Again, in agreement with experiment and also with predictions of previous MF calculations,[3,8,12] the AF phase is characterized by parallel spins residing on the 1-2 dimer (Fig. 2), as can also be inferred from simple arguments based on the dimer picture.[3]

Having developed a simple and efficient method to solve the MF problem for the ET-Y family, we can now play around with parameters trying to gain some information
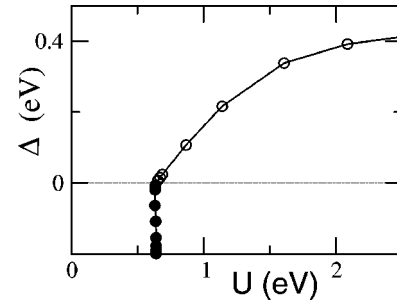

FIG. 5. The conductivity gap (see text) vs U, same parameters as in Fig. 3.
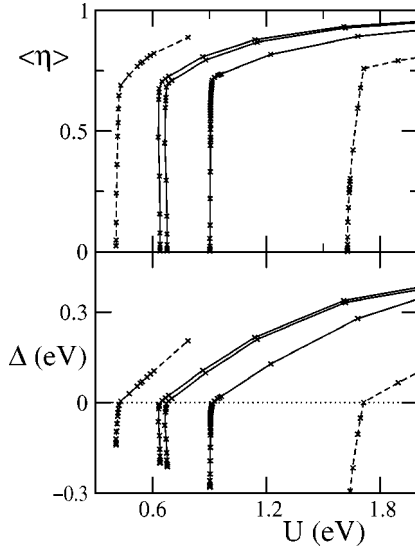
FIG. 6. The AF order parameters and the conductivity gap vs U. Continuous lines refer to t values in Table I for ET-Cl, with p increasing from left to right. Dashed lines refer to nominal pressures $p = -33$ kbar, at left, and $p = 95$ kbar, at right (see text).

about the rich phase diagram of these systems. In Fig. 6 the continuous lines show the U dependence of $\langle \eta_{AF1} \rangle$ and Δ, calculated for the available t's relevant to ET-Cl at $p = 3$ and 27 kbar (Table I). The critical U increases with p from ~ 0.64 eV at $T = 127$ K, ambient p, to ~ 0.68 eV and ~ 0.91 eV, at ambient T and $p = 3$, 27 kbar, respectively. The increase of U_c corresponds to a stabilization of the metallic phase, and can justify the appearance of SC in ET-Cl under pressure, as we shall discuss in more detail in the next section.

In the scale of Fig. 6 the curve relevant to $p = 3$ kbar shows a very narrow region with a negative slope. However, the width of this region is only 2–3 times the numerical uncertainty on U, so that we cannot make any strong statement about observing a discontinuous, first order transition. In any case, the coexistence region, i.e., the hysteresis region for this transition, if present, would be so small to be irrelevant for any practical purpose. The region of negative slope disappears at $p = 27$ kbar, where the transition looks smoother, with possibly a finite positive slope. Once more the effect is tiny and hardly disentangled from numerical uncertainties.

To get some clearer feeling about the role of pressure, we have linearly extrapolated the t estimates available at $p = 3$ and 27 kbar to higher pressures. In Fig. 6 the rightmost dashed line shows the corresponding evolution of the order parameter for a nominal $p = 95$ kbar, where t_q extrapolates to zero. The smoothing of the transition is now evident: in this case $\langle \eta_{AF1} \rangle (U)$ clearly has a well-defined positive slope. An interesting observation is that the conduction gap (lower panel) closes not at the very beginning of the transition, but only when the transition comes to completeness. This corresponds to the appearance of a region of stability for a phase with simultaneously AF distortion and residual metallic behavior. In other words, when the transition is continuous, our

data suggest the presence of an antiferromagnetic metal phase, similar to that discussed at length in Refs. 3, 8, 12. However, the extent of this phase is very narrow, so that it represents at most a transient phase.

Searching for some evidence of discontinuous phase transition, we have also "released the pressure," by extrapolating the t's estimates at $p = 3$ and 27 kbar down to a nominal pressure of -33 kbar. Surprisingly, the transition is continuous again, and smoother than at ambient p. Therefore, we find no clear evidence for discontinuous transitions, except possibly in a very narrow region in the parameter space corresponding to ET-Cl at $p = 3$ kbar. In general, the observation of very narrow regions of discontinuity and/or AF-metallic coexistence is strongly affected by numerical uncertainties and/or finite-size effects.[29] These transient states, being intrinsically unstable, cannot be associated with physically significant states. On the other hand, their presence for particular values of the parameters signals an intrinsic instability of the system to external perturbations, such as those eventually leading to superconductivity.

IV. DISCUSSION

Overall our results agree with previous MF calculations on κ-(BEDT-TTF)$_2$Cu(NCS)$_2$,[3,8,12] describing the transition from a paramagnetic metal to an AF insulator occurring at $U_c \sim 0.6$–0.8 eV (the precise value of course depends on the choice of the t's). However, some details on the evolution of the order parameter and on the opening of the semiconducting gap are different. In the recursive approach to the solution of the MF problem, adopted so far in the literature, the only viable procedure to estimate U_c relies on searching for the minimum U where finite $\langle \eta_{AF1} \rangle$ appears. As discussed above, this procedure leads to large uncertainties in U_c, that have to be properly accounted for in the analysis of numerical results. Kino and Fukuyama[3,12] use very small lattices ($N = 3600$), corresponding to an intrinsic uncertainty in $\langle \eta_{AF1} \rangle$ of at least 4×10^{-4}. In Ref. 3 the onset of AF is estimated to occur at U_{c2}, with $\langle \eta_{AF1} \rangle \sim 0.02$. This small value for the order parameter implies a minimum uncertainty in U_{c2} of ~ 0.02 eV. Then the two transition points observed by Kino and Fukuyama, $U_{c1} = 0.762$ eV and $U_{c2} = 0.758$ eV, coincide within numerical accuracy. In the lack of additional information their data are consistent with a single transition, as we find for the t's relevant to ET-Cl at $T = 127$ K or at $p = 3$ kbar (Fig. 6). The presence of an antiferromagnetic metallic phase is then questionable. Similar problems occur in the interpretation of data in Ref. 12. Here a two-transition scenario is proposed at low p, involving a continuous transition from a paramagnetic metal to an antiferromagnetic metal (finite η_{AF1} and negative Δ), immediately followed by a first order transition to an insulating state. This complex scenario, that we were unable to reproduce in our large lattice for any choice of the parameter set, is probably either a finite-size effect or a numerical artifact. One must also keep in mind the possibility it represents a characteristic feature of κ(BEDT-TTF)$_2$Cu(NCS)$_2$, due to its lower symmetry. However, since it does not appear in the more symmetric

ET-Cl phase at any pressure, it is irrelevant as far as SC is concerned.

In Ref. 8 the numerical uncertainty in $\langle n_{i\uparrow} \rangle$, fixed by the authors at 0.001, propagates to give $\delta \langle \eta_{AF1} \rangle \sim 0.0014$. As a consequence, the estimate for U_a, i.e., the critical U for the appearance of AF order, obtained for $\langle \eta_{AF1} \rangle = 0.01$, is affected by a large uncertainty: $U_a = 0.7 \pm 0.1$ eV. More precise estimates are obtained for larger $\langle \eta_{AF1} \rangle$, e.g., $U_c = 0.685$ is essentially constant for $\langle \eta_{AF1} \rangle = 0.037, 0.499, 0.582$, representing a good estimate for the critical U where AF order appears and, at the same time, the electronic orbits close. The proposed estimate of the critical U for the opening of the semiconducting gap, $U_i = 0.699 \pm 0.001$ is different from U_c, again suggesting the presence of an intermediate phase with both metallic and AF character. Quite in agreement with our results at large p, the metallic antiferromagnetic phase is a marginal phase that only survives in a very narrow transient regime. Indeed, as pointed out in Ref. 30 (Sec. 3.4.5), such a phase would imply a weak AF order and reconstruction of the Fermi surface, which, however, have not been experimentally observed. Our approach thus proves useful in excluding on a purely theoretical basis the spurious complexities in the phase diagram due to finite-size effects and/or numerical uncertainties, and should be particularly convenient when extended to describe charge ordering instabilities together with magnetic instabilities.

Several papers discuss κ-phase BEDT-TTF salts within the dimer approximation.[3,5,18,19] Basically, the tight-binding Hamiltonian for the four frontier molecular orbitals in the unit cell is rewritten in terms of the bonding and antibonding orbitals of the t_{b1} dimers. Since t_{b1} is at least twice as large as the other hopping integrals, the interactions between bonding and antibonding orbitals are neglected, and the original four-bands problem reduces to a two-band problem. In the resulting lattice each site has four nearest-neighbor sites, interacting through $(t_p + t_q)/2$, and two next nearest-neighbors, interacting with $t_{b2}/2$. For the parameters relevant to k-phase salts, the bands calculated within the dimer model compare favorably with those obtained in the four-band calculation, confirming the validity of the dimer model approximation at least for the noninteracting case.[19] The dimer-model lattice is simple, but still shows interesting physics. In fact, by varying the $(t_p + t_q)/t_{b2}$ ratio, it interpolates between a square lattice and a collection of 1D chains.[21] Whereas it is suggestive to relate the variegated behavior obtained from such a model to the variety of observed properties for κ-phase salts, some caution is in order. Just as an example, consider the case $t_{b2} \rightarrow 0$, where the dimer lattice reduces to a half-filled square lattice with perfect nesting. As it is well known, the critical U for the antiferromagnetic instability goes to zero in this limit, as also confirmed by MF calculations.[10] Instead, a MF calculation for the same parameters as in Fig. 3, but $t_{b2} = 0$, yields a continuous transition to the AF phase with a finite and fairly large $U_c \sim 0.57$ eV. This qualitatively different behavior can be easily rationalized: The small interactions between bonding and antibonding orbitals are large enough to break the commensurability of the simple dimer model at $t_{b2} = 0$.[10,21] A word of caution is also necessary when introducing electron correlations in the dimer model. Indeed, starting from a Hubbard Hamiltonian for the four-molecules layer, the resulting effective U_{dim} for the dimer model is related to both U and t_{b1}, according to a relation first proposed in Ref. 3 and rediscussed and extended in Ref. 5. For the commonly accepted value of $U \sim 4t_{b1}$, U_{dim} is of the order of t_{b1}.[5] Thus the applicability of FLEX and perturbative approaches[15–17] to the dimer model becomes questionable, since these approaches work well in the limit $U_{dim} \sim t_{b1} \ll (t_p + t_q)/2, t_{b2}/2$, where the dimer model itself breaks down.

We now relate our results to the experimental observations relevant to the ET-Y family. As mentioned above, several evidences indicates that the ET-Y salts are just at the AF/SC borderline. At ambient pressure the ET-Cl salt is a Mott antiferromagnet, with a magnetic moment amplitude of $0.45 \mu_B$,[31] that compares favorably with the present and previous[3,8,12] estimates of the magnetic order parameter. By applying pressure above 300 bar, ET-Cl shows a transition to complete superconductivity at about 12 K. At lower pressures, reentrant and partial superconductivity, with residual sample resistance, have been observed.[32] The fully deuterated ET-Cl (d_8-ET-Cl) exhibits analogous behavior, only requiring a slightly higher pressure (440 bar) to reach superconductivity.[32] ET-Br is superconducting at ambient pressure ($T_c \sim 11$ K) but the attainment of the superconducting phase is affected both by the cooling rate and by the deuteration of the sample.[33] It has been shown that by keeping constant the cooling rate at a sufficiently low value, the partially deuterated d_2- and d_4-ET-Br salts are superconducting at practically the same T_c as the undeuterated sample. The d_6-salt, on the other hand, exhibits a complicated behavior attributed to the competition between superconducting and insulating phase.[33] Finally, the fully deuterated d_8-ET-Br is an antiferromagnetic insulator (magnetic moment $0.3 \mu_B$),[31] and under pressure has a behavior similar to ET-Cl, reaching complete superconductivity just above 60 bar.[34] For the sake of completeness, we mention that the ET-I salt is not superconducting, even when pressures up to 5 Kbar are applied.[23] This kind of behavior has been ascribed to disorder. However, this compound is the least investigated in the ET-Y family, and we shall not consider it here.

Rather obviously, a MF approach is inadequate to describe phenomena related to non-equilibrium states, disorder and/or sample inhomogeneity, such as cooling rate effects and reentrant superconductivity. We therefore focus here on the complete-SC/AF crossover affected by pressure and/or by isotopic substitution. The universal phase diagram in Fig. 1 presents the parameter "pressure" as the abscissa. It has been used to explain the differences induced by the Cl-Br substitution or deuteration in ET-Y salts, and similar effects. In particular, the smaller radius of Cl$^-$ with respect to Br$^-$ implies a reduced effective pressure[1] in ET-Cl with respect to ET-Br (see Ref. 2 for a tentative numerical assessment of this effect). A similar effect of reduced pressure can be associated to deuteration, which corresponds to smaller end-group excursions around their equilibrium values. From the values of the corresponding T_c's, we can empirically associate an increase in p of ~ 380 bar for the Cl-Br substitution, and a decrease of ~ 140 bar for deuteration. A rationalization
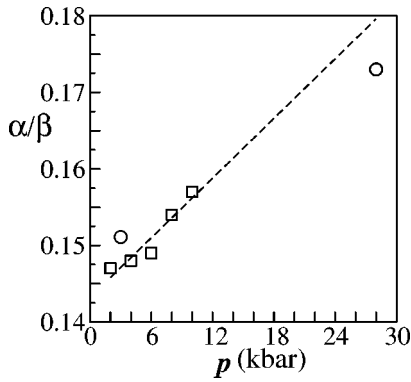
FIG. 7. Pressure dependence of the ratio between the areas of α and β orbits in the ac plane Fermi surface. The squares refer to the experimental data (Ref. 35), with the dashed line representing the best linear fit. Circles are the calculated values for ET-Cl data in Table I.

of these tiny effects is fairly difficult. We shall examine below whether our MF results help in this respect.

We first focus on ET-Cl. The hopping integrals in the ac plane, calculated for the known crystal structures at ambient p and 127 K,[23] and at 3 and 28 kbar (ambient T)[24] are reported in Table I. To make a first comparison with experiment, we have evaluated the areas of the α and β orbits from the ac plane Fermi surface calculated in the tight binding approximation. The results relevant to the metallic phase are compared in Fig. 7 with the measured areas from Shubnikov–de Haas (SdH) experiments performed at several pressures in the 2–10 kbar range at the liquid helium temperature.[35] In order to renormalize the effects associated to the global volume contraction due to the different temperatures of the SdH and structural data, the α/β ratio has been reported as a function of pressure. In fact, the β area is equal to the area of the Brillouin zone for the 3/4-filled system. The 3 kbar α/β nicely fits the experiment, and a straight line through the experimental points extrapolates near to the calculated 28 kbar point. We notice that the crystallographic axes ratio c/a is practically unchanged with pressure.[24] This observation sheds doubts on the possibility of adopting c/a as a rough estimate of α/β, as suggested by Ref. 2.

Table I, rightmost column, reports the ET-Cl U_c values calculated by our MF approach. A word of warning is necessary when comparing data obtained at different temperatures, since it has been observed[36] that the values of the hopping parameters change correspondingly. However, this effect is not very pronounced in ET-Y family,[2,36] and we shall neglect it in the following. We notice that U_c increases monotonously with p, thus accounting for the pressure driven superconductivity transition in terms of an increase of the critical value needed to reach the AF phase. In this respect, U_c seems to be a good ''indicator'' of the effective pressure of Fig. 1. Other previously suggested indicators, such as the t_{b1}/t_p ratio,[3,12] or the c/a ratio,[2] seem to work less satisfactorily in this case: t_{b1}/t_p does not increase monotonously

with p (Table I), and, as noted above, c/a is practically constant.

We now turn attention to ET-Br. When comparing the ambient pressure, 127 K hopping integrals of ET-Cl with the corresponding ones of ET-Br, one finds small differences, and we get for the two systems virtually identical phase transitions, occurring at basically the same U_c (Table I). Therefore, the different ground state of ET-Cl (AF) and ET-Br (SC) at ambient pressure cannot be understood in terms of a difference in U_c. One might think that the actual effective U is different in the two types of salts, being smaller in ET-Br due a larger screening of the intersite Coulomb potential from the more polarizable Br anions. However, this kind of qualitative explanation is not corroborated by the numerical values of the anion polarizabilities obtained from *ab initio* calculations,[37] and is difficult to reconcile with the observation of an AF state for d_8-ET-Br at ambient pressure. We could not calculate the hopping integrals in this case, as the atomic coordinates are not available in the literature. We have used the t's calculated in Ref. 36 for both ET-Br and d_8-ET-Br at 127 K (properly rescaled since the method of calculation is different from ours). We do not find significant difference between the U_c's of the two compounds.

As we already pointed out, c/a and t_{b1}/t_p are not good indicators of the properties of κ-phase salts, and cannot be chosen as the x-axis parameter in a *universal* phase diagram similar to that reported in Fig. 1. Both the ratio of α and β orbits and U_c work satisfactorily as far as the p dependence of ET-Cl properties is concerned. However, both fail if applied to rationalize the different behavior of ET-Cl and ET-Br and/or the effects due to deuteration. It is important to underline that both α/β and U_c are ''single particle'' parameters, in the sense that they are fully determined by the band structure, i.e., the t's values. Investigating the band structure of κ-phase salts offers useful information to rationalize their behavior, but this information is not enough, and the role of interactions beyond single-particle picture has to be invoked to understand the behavior of systems near the AF/SC interface. The failure of simple band-structure treatments for κ-phase salts has been recently suggested based on the p dependence of cyclotron effective masses with pressure,[25] and can also be recognized from high resolution measurements of thermal expansion coefficients.[38] Residual electronic correlations, disorder induced localization effects, electron-phonon coupling, and interlayer effects all can play an important role, particularly at the AF/SC interface. More theoretical and experimental work is in order to settle the relative importance of these effects.

ACKNOWLEDGMENTS

[1] R.H. McKenzie, Science **278**, 820 (1997), and references therein.

[2] T. Mori, H. Mori, and S. Tanaka, Bull. Chem. Soc. Jpn. **72**, 179 (1999).

[3] H. Kino and H. Fukuyama, J. Phys. Soc. Jpn. **64**, 2726 (1995).

[4] K. Kanoda, Hyperfine Interact. **104**, 235 (1997).

[5] R.H. McKenzie, Comments Condens. Matter Phys. **18**, 309 (1998).

[6] J. Schmalian, Phys. Rev. Lett. **81**, 4232 (1998).

[7] V.A. Ivanov, E.A. Ugolkova, and M.E. Zhuralev, JETP **86**, 395 (1998).

[8] E. Demiralp and W.A. Goddard III, Phys. Rev. B **56**, 11 907 (1997).

[9] Y. Imamura, S. Ten-no, K. Yonemitsu, and Y. Tanimura, J. Chem. Phys. **111**, 5986 (1999), and references therein.

[10] G. Visentini, A. Painelli, and A. Fortunelli, Synth. Met. **103**, 1993 (1999).

[11] H. Seo, J. Phys. Soc. Jpn. **69**, 805 (2000).

[12] H. Kino and H. Fukuyama, J. Phys. Soc. Jpn. **65**, 2158 (1996).

[13] J.M. Williams, J.R. Ferraro, R.J. Thorn, K.D. Carlson, U. Geiser, H.H. Wang, A.M. Kini, and M.-H. Whangbo, *Organic Superconductors (Including Fullerenes)* (Prentice Hall, Englewood Cliffs, NJ 1992).

[14] J.M. Williams, A.J. Schultz, U. Geiser, K.D. Carlson, A. M. Kini, H.H. Wang, W.-K. Kwok, M.-H. Whangbo, and J.E. Shirber, Science **252**, 1501 (1991).

[15] H. Kino and H. Kontani, J. Phys. Soc. Jpn. **67**, 3691 (1998).

[16] H. Kondo and T. Moriya, J. Phys. Soc. Jpn. **67**, 3695 (1998).

[17] T. Jujo, S. Koikegami, and K. Yamada, J. Phys. Soc. Jpn. **68**, 1331 (1999).

[18] J. Caufield, W. Lubczynski, F.L. Pratt, J. Singleton, D.Y.K. Ko, W. Hayes, M. Kurmoo, and P. Day, J. Phys.: Condens. Matter **6**, 2911 (1994).

[19] G. Visentini, A. Painelli, A. Girlando, and A. Fortunelli, Europhys. Lett. **42**, 467 (1998).

[20] W. Hofstetter and D. Vollhardt, Ann. Phys. (Leipzig) **7**, 48 (1998).

[21] S-W Tsai and J.B. Marston, cond-mat/0010300 (unpublished).

[22] S. Mazumdar, R.T. Clay, and D.K. Campbell, Phys. Rev. B **62**, 13 400 (2000).

[23] U. Geiser, A.J. Schultz, H.H. Wang, D.M. Watkins, D.L. Stupka, J.M. Williams, J.E. Schirber, D.L. Overmyer, D. Jung, J.J. Novoa, and M.-H. Whangbo, Physica C **174**, 475 (1991).

[24] A.J. Schultz, U. Geiser, H.H. Wang, J.M. Williams, L.W. Finger, and R.M. Hazen, Physica C **208**, 277 (1993); A.J. Schultz, H.H. Wang, J.M. Williams, L.W. Finger, R.M. Hazen, C. Rovira, and M-H Whangbo, *ibid.* **234**, 200 (1994).

[25] J. Merino and R.H. McKenzie, Phys. Rev. B **62**, 2416 (2000).

[26] A. Fortunelli and A. Painelli, Phys. Rev. B **55**, 16 088 (1997); J. Chem. Phys. **106**, 8051 (1997).

[27] A. Painelli and A. Girlando, Phys. Rev. B **37**, 5748 (1988).

[28] G. Visentini, M. Masino, C. Bellitto, and A. Girlando, Phys. Rev. B **58**, 9460 (1998); J. Singleton, F.L. Pratt, M. Doporto, T.J. Janssen, M. Kurmoo, J.A.A.J. Perenboom, W. Hayes, and P. Day, Phys. Rev. Lett. **68**, 2500 (1992); U. Mayaffre, P. Wzietek, C. Lenoir, D. Jerome, and P. Batail, Europhys. Lett. **28**, 205 (1994).

[29] V.E. Korepin, N.M. Bogoliubov, and A.G. Izergin, *Quantum Inverse Scattering Method and Correlation Functions* (Cambridge University Press, Cambridge, 1993).

[30] J. Singleton, Rep. Prog. Phys. **63**, 1111 (2000).

[31] K. Miyagawa, A. Kawamoto, K. Uchida, and K. Kanoda, Physica B **284-288**, 1589 (2000).

[32] H. Ito, T. Ishiguro, M. Kubota, and G. Saito, J. Phys. Soc. Jpn. **65**, 2987 (1996).

[33] H. Taniguchi, A. Kawamoto, and K. Kanoda, Physica B **284-288**, 519 (2000).

[34] H. Ito, T. Ishiguro, T. Kondo, and G. Saito, J. Phys. Soc. Jpn. **69**, 290 (2000).

[35] M.V. Kartsovnik, G.Yu. Logvenov, H. Ito, T. Ishiguro, and G. Saito, Phys. Rev. B **52**, 15 715 (1995); Synth. Met. **85**, 1471 (1997); M.V. Kartsovnik, W. Biberacher, K. Andres, and N.D. Kushch, JETP Lett. **62**, 905 (1995); H. Weiss, M.V. Kartsovnik, W. Biberacher, E. Steep, A.G.M. Jansen, and N.D. Kushch, *ibid.* **66**, 202 (1997).

[36] M. Watanabe, Y. Nogami, K. Oshima, H. Ito, T. Ishiguro, and G. Saito, Synth. Met. **103**, 1909 (1999).

[37] A. Fortunelli (unpublished).

[38] J. Muller, M. Lang, J.A. Schlueter, U. Geiser, and D. Schweitzer, Synth. Met. **120**, 855 (2001).